Carnegie Observatories Astrophysics Series, Vol. 4:
Origin and Evolution of the Elements, 2004
ed. A. McWilliam and M. Rauch (Cambridge: Cambridge Univ. Press)

The Impact of Rotation on Chemical Abundances in Red Giant Branch Stars

CORINNE CHARBONNEL
Geneva Observatory, 1290 Sauverny, Switzerland
LA-OMP (CNRS UMR 5572), 14, av.E.Belin, 31400 Toulouse, France

Abstract

Low-mass stars ($<$2–2.5 $M_\odot$) exhibit, at all the stages of their evolution, signatures of processes that require challenging modeling beyond the standard stellar theory. In this paper we focus on their peculiarities while they climb the red giant branch (RGB). We first compare the classical predictions for abundance variations due to the first dredge-up with observational data in various environments. We show how clear spectroscopic diagnostics probe the nucleosynthesis and the internal mixing mechanisms that drive RGB stars. Coherent data reveal in particular the existence of a nonstandard and shallow mixing process that changes their surface abundances at the so-called RGB bump. We show that the occurrence of this extra-mixing process is certainly related to rotation. Finally we discuss the so-called Li-flash, which is expected to occur at the very beginning of the extra-mixing episode.

1.1 Abundance Anomalies in RGB Stars Due to *In Situ* Processes

1.1.1 Abundance Variations in RGB Stars Due to the First Dredge-up

According to the classical stellar evolution theory*, the only opportunity for low-mass stars to modify their surface abundances happens on their way to the red giant branch (RGB) when they undergo the so-called first dredge-up (Iben 1965). During this event their convective envelope deepens in mass, leading to the dilution of the surface pristine material within regions that have undergone partial nuclear processing on the main sequence. Qualitatively, this leads to the decrease of the surface abundances of the fragile Li, Be, and B elements and of ^{12}C, while those of ^{3}He, ^{13}C, and ^{14}N increase. Due to low temperatures inside main sequence low-mass stars, O and heavier elements are not affected by nuclear reactions, and their surface abundances remain unchanged subsequent to the first dredge-up. Quantitatively, the abundance variations due to the first dredge-up depend on the stellar mass and metallicity (e.g., Sweigart, Greggio, & Renzini 1989; Charbonnel 1994; Boothroyd & Sackmann 1999). After the first dredge-up, the convective envelope withdraws while the hydrogen-burning shell moves outwards in mass. No more variations of the surface abundances are then expected until the star reaches the asymptotic giant branch.

* By this we refer to the modeling of nonrotating, nonmagnetic stars, in which convection is the only mixing process considered.

1.1.2 Observational Clues of a Second Mixing Episode on the RGB

The first dredge-up predictions agree with the observations on the lower part of the RGB†. However, observational evidences have accumulated, that we list below, of a second and distinct mixing episode that occurs in low-mass stars after the end of the first dredge-up, and more precisely at the RGB bump.

The determination of the carbon isotopic ratio (^{12}C/^{13}C) for RGB stars in open clusters with various turn-off masses (Gilroy 1989) provided the first pertinent clue on this process. It was indeed shown that bright RGB stars with initial masses lower than $\sim$2–2.5 $M_\odot$ exhibit carbon isotopic ratios considerably lower than predicted by the first dredge-up. Thanks to data in stars sampling the RGB of M67 (Gilroy & Brown 1991), it clearly appeared that observations deviated from classical predictions just at the so-called RGB bump (Charbonnel 1994). Field and globular cluster stars behave similarly*. In the former case this could be established thanks to the determination of the carbon isotopic ratio in large samples of stars for which *Hipparcos* parallaxes allowed the precise determination of their evolutionary status (Charbonnel, Brown, & Wallerstein 1998; Gratton et al. 2000). We knew for a long time that the brightest RGB stars in globular clusters presented carbon isotopic ratios close to the equilibrium value. But very recently the region around the bump could finally be probed for two globular clusters: In NGC 6528 and M4, the carbon isotopic ratio drops below the first dredge-up predictions just at the RGB bump (Shetrone 2003).

The extra-mixing process affects the surface abundances of other chemical elements: Li also decreases at the RGB bump, both in the field and in globular clusters (Pilachowski, Sneden, & Booth 1993; Grundahl et al. 2002). In field stars C decreases, while N increases for RGB stars brighter than the bump (Gratton et al. 2000), confirming the CN processing of the stellar envelope. The lowering of the C abundance along the RGB is also seen in globular clusters (e.g., Bellman et al. 2001, and references therein), though in this case the picture is more confused because of a probable nonnegligible dispersion of the initial [C/Fe].

An *in situ* mechanism has also frequently been invoked to explain the abundance anomalies of heavier elements in globular cluster stars, and in particular the O-Na anticorrelation. This pattern has been observed in the brightest globular cluster RGB stars for a long time (see references in Ivans et al. 1999 and Ramírez & Cohen 2002). However, it is only thanks to 8–10 m-class telescopes that O and Na abundances could be determined for less evolved stars, and in particular for turn-off stars in a couple of globular clusters (Gratton et al. 2001; Thévenin et al. 2001; Ramírez & Cohen 2002). There, the O-Na anticorrelation extends to the main sequence. This result is crucial. Indeed, the ON- and NeNa-cycles do not occur in main sequence low-mass stars, as the involved reactions require too high temperatures that are only reached when low-mass stars are on the RGB. Thus, the fact that the O-Na anticorrelation already exists on the main sequence clearly proves that it is not produced by *in situ* processes, but by external causes, the discussion of which is out of the scope of this paper (see Charbonnel 2004).

Recently we have searched for an eventual evolution of the O and Na abundances with luminosity along the RGB for field stars. We gathered from the literature a large sample (625) of field stars with *Hipparcos* parallaxes over a large range of metallicity ([Fe/H] between

† One has, of course, to take into account possible variations of the surface Li abundance occurring already on the main sequence. This discussion is, however, out of the scope of the present paper.

* The literature on the various abundance anomalies within globular clusters is so large that we chose to quote here only the most recent papers to illustrate our discussion.

−2.5 and 0) for which we homogeneously redetermined the abundances of a large number of elements. No evolutionary effect could be found, neither for O nor Na (Palacios et al. 2002; Charbonnel et al. 2004), in agreement with the most recent globular cluster data mentioned above [see also Yong et al. (2003, 2004) for a discussion on Mg and Al].

Last, but not least, the recent determination of the oxygen isotopic ratios in a couple of RGB stars with low carbon isotopic ratios (Balachandran & Carr 2004) confirmed this result. In these objects, indeed, both the $^{16}O/^{17}O$ and $^{16}O/^{18}O$ ratios appear to be high, in agreement with extensive CN-processing but no dredge-up of ON-cycle material in RGB stars (see the arrow in Fig. 1.1).

1.2 Origin and Nature of the Extra-mixing Process

The observations summarized previously provide definitive clues on a second and distinct mixing episode that occurs in low-mass stars well after the end of the first dredge-up, precisely at the RGB bump. This process appears to be universal: it affects more than 95% of the low-mass stars (Charbonnel & do Nascimento 1998), whether they belong to the field, to open, or to globular clusters. Its signatures in terms of abundance anomalies are clear: the Li and the ^{12}C abundances as well as the $^{12}C/^{13}C$ ratio drop, while the ^{14}N abundance and the $^{16}O/^{18}O$ ratio increase. On the other hand ^{16}O, ^{17}O, Na, and heavier elements remain unaffected. As we shall see in §1.4, this sequence may start with a very brief episode of Li enrichment.

These coherent data indicate that during the extra-mixing episode at the RGB bump, the stellar convective envelope is connected with the radiative regions where CN-burning occurs, but not with the ON- and NeNa-processed layers (see Fig. 1.1). The important increase of the molecular weight (or μ) gradients when one approaches the hydrogen-burning shell certainly shields these deeper regions from the extra-mixing.

μ-gradients are also certainly responsible for the fact that the extra-mixing starts to be efficient only at the RGB bump. Indeed, during the first dredge-up a μ-discontinuity is built at the region of the deepest penetration of the convective envelope. This μ-barrier then probably inhibits any mixing between the convective envelope and the hydrogen-burning shell. At the RGB bump, the external regions of the hydrogen-burning shell pass through the μ-discontinuity*. From the mixing point of view, after this evolutionary point the μ-gradients between the base of the convective envelope and the hydrogen-burning shell are much smoother, allowing the occurrence of some extra-mixing in this radiative region (Sweigart & Mengel 1979; Charbonnel 1994, 1995; Charbonnel et al. 1998).

All these observational facts represent strong clues on the origin of the extra-mixing process, which is certainly rotationally induced. Indeed, μ-gradients have been known for a long time to be powerful in inhibiting meridional circulation (Mestel 1953, 1957).

1.3 Rotation-induced Mixing

Sweigart & Mengel (1979) investigated the possibility that meridional circulation might lead to the mixing of CNO-processed material in RGB stars. Since then, a lot of work

* Due to the composition changes in the burning region, the stellar structure has to readjust, and the stellar luminosity then slightly decreases before increasing again. Low-mass stars spend a nonnegligible part of their RGB lifetime in this region; this explains why the bump clearly appears as a peak in the differential luminosity function of the Galactic globular clusters or as a change in the slope of the cumulative luminosity function (e.g., Zoccali et al. 1999).

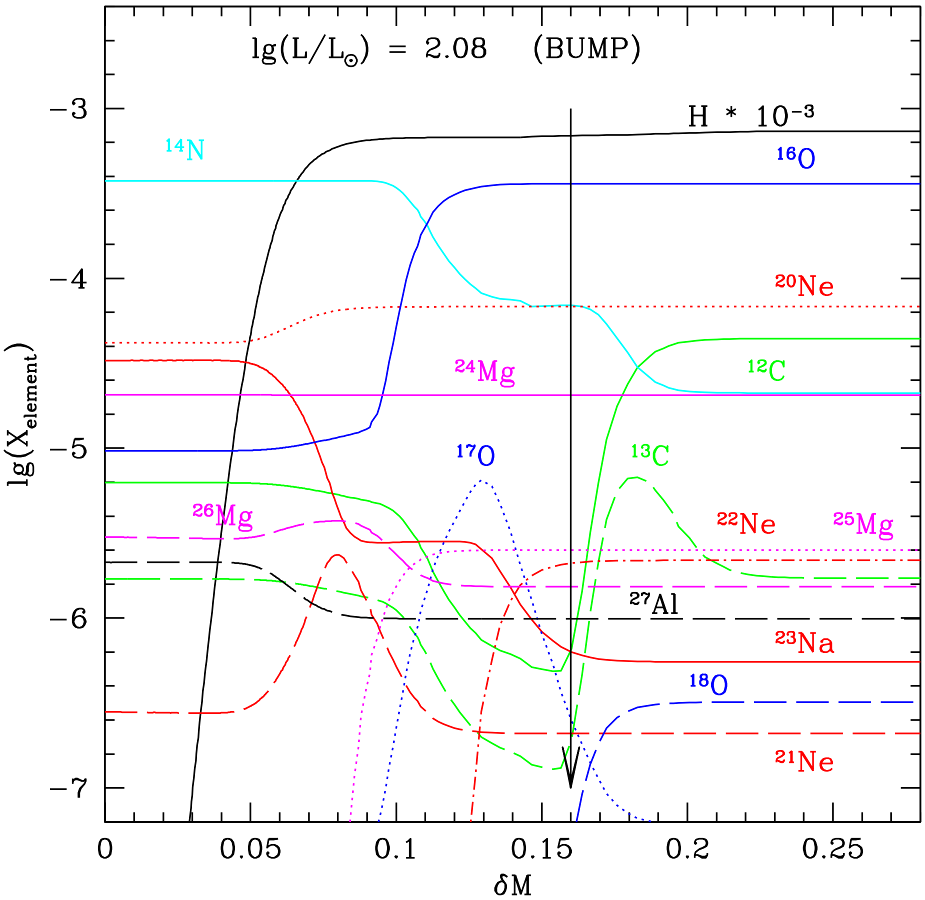

Fig. 1.1. Abundance profiles of the isotopes participating in the CNO, NeNa, and MgAl cycles inside a 0.83 $M_\odot$, [Fe/H]= −1.6 (typical of the globular cluster M13) standard model at the luminosity of the RGB bump. The abscissa is the relative mass coordinate, $\delta M = (m_r - m_{BHBS})/(m_{BCE} - m_{BHBS})$, where m_r is the mass within a given radius, m_{BHBS} is the mass at the bottom of the hydrogen-burning shell, and m_{BCE} is the mass at the base of the convective envelope; $\delta M = 0$ at the bottom of the hydrogen-burning shell and $\delta M = 1$ at the base of the convective envelope. The vertical arrow indicates the maximum depth down to which the extra-mixing process is efficient according to the observations.

has been done on the physics of the mixing induced by rotation. Zahn (1992) proposed a description of the interaction between meridional circulation and shear turbulence, pushing forward the idea of choking of meridional circulation by μ-gradients. Following these developments, Charbonnel (1995) showed that such a process can indeed account for the observed behavior of carbon isotopic ratios and for the Li abundances in Population II low-mass giants. Simultaneously, when this extra-mixing begins to act, ^{3}He is rapidly transported down to the regions where it burns by the ^{3}He$(\alpha,\gamma)^7$Be reaction. This leads to a decrease of the surface value of ^{3}He/H, solving the long-standing problem of the Galactic evolution of ^{3}He (e.g., Charbonnel 2002).

In these exploratory computations, however, the transport of angular momentum by the hydrodynamical processes was not treated self-consistently, though it is of utmost importance in the understanding of rotation-induced mixing. Let us now discuss the results obtained for RGB stars when the transport of angular momentum and of the chemicals, as described by Zahn (1992) and latter on by Talon et al. (1997), Maeder & Zahn (1998), and Palacios et al. (2003), is taken into account.

Two independent studies have been carried out using basically the same physical description of rotational mixing: Denissenkov & Tout (2000) and Palacios, Talon, & Charbonnel (2004). They differ on some details of the input physics, such as the choice of the shear instability criteria and of the expression of the diffusion coefficient associated with vertical turbulence. But more importantly, a drastic assumption differentiates both studies: Denissenkov & Tout (2000) indeed compute the transport of angular momentum and of the chemicals in a post-processing way; in other words, they use the internal structure of a few *standard* RGB models to estimate the mixing efficiency and the corresponding changes in the surface abundances. In this approach, there is no feedback of the mixing on the stellar structure and evolution, which are computed independently.

On the other hand, Palacios et al. (2004) treat in a self-consistent way the transport of angular momentum and of the chemicals inside their stellar evolution code, thereby following the "nonstandard" evolution from the zero-age main sequence on. As a result, in this case the mixing has a feedback on the star since its early evolution. On the RGB, in particular, the mixing distorts the stationary profiles of the chemicals deep inside the star even if the surface abundances are not yet affected. In turn, the mixed star reacts to the mixing that it undergoes, thereby influencing the mixing itself (see §1.4).

This difference has a strong impact on the final predictions. In Denissenkov & Tout (2000), indeed, the mixing is applied to standard profiles, and surface variations of O and Na are predicted in RGB stars. In Palacios et al. (2004), however, the mixing is applied on self-consistently distorted profiles; as a result, hardly any variation of even the C and N isotopes is produced at the stellar surface by this process alone. One could thus question the actual role of rotation in this problem. However, something crucial happens, that we discuss below.

1.4 The Li Flash

A few ($\sim 1\%$) RGB stars present Li overabundances. The fact that these so-called super Li-rich giants are all located at the RGB bump and still exhibit "standard" carbon isotopic ratios led Charbonnel & Balachandran (2000) to conclude that the Li-rich phase was a precursor to the extra-mixing process described previously. This brought very tight constraints on the underlying physics. Indeed, the transport coefficient D_R obtained in the case of rotation-induced mixing are also too low to lead to surface lithium enrichment.

Palacios, Charbonnel, & Forestini (2001) proposed that the structural response to the mixing could actually be the cause of the increase of D_R, which is necessary to produce super Li-rich giants and to change the surface abundances of other elements. The mixing sequence is the following. At the RGB bump the external wing of the ^{7}Be peak crosses the molecular weight discontinuity before the ^{13}C peak does, and is then connected with the convective envelope by the extra-mixing process. ^{7}Be produced via ^{3}He$(\alpha,\gamma)^7$Be starts to diffuse outwards. However, due to the relatively low D_R given above, the transported ^{7}Be decays to ^{7}Li in regions where the ^{7}Li is rapidly destroyed by proton capture. A lithium-burning shell appears. ^{7}Li(p,α)α becomes the dominant reaction, leading to an increase of the local temperature and of both the local and total luminosities.

Palacios et al. suggested that the meridional circulation and the corresponding transport coefficient then increase due to the $\epsilon_{\rm nuc}$(^{7}Li+p) burst, allowing for lithium enrichment of the convective envelope. Indeed, in the developments for the transport of matter and angular momentum, the effective diffusivity is proportional to $[rU(r)]^2$, the vertical component of the meridional velocity. This quantity is itself proportional to terms that depend on both the velocity profile and the chemical inhomogeneities along isobars (see Maeder & Zahn 1998 for the complete expressions). But what is important for the present discussion is their dependence on the local rates of nuclear and gravothermal energies. We thus proposed that the apparition of the Li-burning shell and the significant release of $\epsilon_{\rm nuc}$(^{7}Li+p) do highly enhance the meridional velocity and the associated transport coefficient as required for the surface lithium abundance to increase.

A lithium flash terminates this phase. As the convective instability develops around the Li-burning shell, it erases the molecular weight gradient and the mixing is free to proceed deeper with higher D_R than initially. Once it reaches the regions where ^{12}C is converted into ^{13}C (as is observed to occur in low-mass stars after the bump) the surface material is exposed to temperatures higher than lithium can withstand. The freshly synthesized lithium is then destroyed as the surface carbon isotopic ratio decreases and the lithium-rich phase ends. This is consistent with the available data on ^{12}C/^{13}C in the lithium-rich RGB stars: those with the highest lithium abundance still have a standard (i.e. post-dredge-up) carbon isotopic value, but no star retains its peak lithium abundance once its carbon isotopic value dips (Charbonnel & Balachandran 2000). When the flash is quenched, the external convective envelope deepens again. We suggest that this creates a new μ-barrier, similar to that built up during the first dredge-up, which then inhibits again the extra-mixing during the subsequent evolution.

We thus have at hand an extra-mixing process that is induced by rotation, but that becomes highly efficient at the RGB bump due to the important release of nuclear energy inside a Li-burning shell. We can thus explain in a self-consistent way the fact that the mixing episode starts by a short period of Li enrichment, followed by a decrease of the fresh Li and of the carbon isotopic ratio. The subsequent deepening of the convective envelope creates a new μ-barrier that will inhibit further mixing after the bump episode.

In order to estimate the time scale of our process, let us define the beginning and the end of the lithium-rich phase, respectively, as the moments where the surface lithium abundance increases above its post-dredge-up value and where the carbon isotopic ratio decreases below its post-dredge-up value. While the duration of the lithium flash itself is quite short ($\sim 2 \times 10^4$ yr in a 1.5 $M_\odot$ solar-metallicity model), the lithium-rich phase so-defined lasts for $\sim$ 60% (i.e. $\sim 6 \times 10^6$ yr) of the classical bump duration. This has to be compared with the number of stars located in the bump region that still present a post-dredge-up carbon isotopic ratio. Among the sample of stars with *Hipparcos* parallaxes and carbon isotopic ratio determinations used in Charbonnel & do Nascimento (1998), $\sim$ 35% of the 49 objects located close to the bump do satisfy this criterion. We consider that this comparison is very encouraging in view of the limited observational sample. This preliminary estimation indicates that many lithium-rich stars should be discovered by observational programs focusing on the bump region.

During the whole sequence described above the temporary increase of the stellar luminosity causes an enhanced mass loss rate, which naturally accounts for the dust shell suggested by the far-infrared color excesses measured for some lithium-rich objects from *IRAS* fluxes (e.g., de la Reza, Drake, & da Silva 1996). Let us note that the contribution of these stars to the lithium enrichment of the Galaxy should be very modest.

1.5 Conclusions

During the last three decades, an incredible amount of work has been devoted to the understanding of the chemical anomalies exhibited by evolved low-mass stars. On the observational side, crucial breakthroughs were made possible recently thanks to the advent of 8–10 m-class telescopes. The signatures of the extra-mixing process that occurs at the RGB bump are now very clear.

On the other hand, recent theoretical models include a sophisticated description of the mixing processes induced by rotation. Those that consistently couple the transport of angular momentum and of the chemicals with the structural evolution of the star predict a Li flash and surface abundance variations on the RGB, in agreement with the observational data. However, a couple of assumptions remain to be tested, in particular the reaction of the meridional circulation and of the various instabilities to a major and local release of nuclear energy.

Rotation-induced mixing processes modify all the stellar outputs, and in particular the final yields from low-mass stars (i.e., ^{3}He is not overproduced anymore by rotating low-mass stars). Their impacts on the stellar lifetimes and on the further evolution (luminosity of the RGB tip, morphology of the horizontal branch, asymptotic giant branch phase, ...) have to be investigated now in a systematic way. This is of crucial importance if one wants to correctly understand the role of low-mass stars in the evolution (chemical and spectrophotometric) of stellar clusters and of galaxies in general.

Acknowledgements. We thank the French Programme National de Physique Stellaire and Programme National Galaxies for their support on this work.

References

Balachandran, S. C., & Carr, J. S. 2004, in CNO in the Universe, ed. C. Charbonnel, D. Schaerer, & G. Meynet (San Francisco: ASP), in press
Bellman, S., Briley, M. M., Smith, G. H., & Claver, C. F. 2001, PASP, 113, 326
Boothroyd, A. I., & Sackmann, I. J. 1999, ApJ, 510, 232
Charbonnel, C. 1994, A&A, 282, 811
——. 1995, ApJ, 543, L41
——. 2002, Nature, 415, 27
——. 2004, in CNO in the Universe, ed. C. Charbonnel, D. Schaerer, & G. Meynet (San Francisco: ASP), in press
Charbonnel, C., & Balachandran, S. 2000, A&A, 359, 563
Charbonnel, C., Brown, J. A., & Wallerstein, G. 1998, A&A, 332, 204
Charbonnel, C., & do Nascimento, J. 1998, A&A, 336, 915
Charbonnel, C., Palacios, A., Thévenin, F., & Bolmont, J. 2004, in preparation
de la Reza, R., Drake, N. A., & da Silva, L. 1996, ApJ, 456, L115
Denissenkov, P. A., & Tout, C. A. 2000, MNRAS, 316, 395
Gilroy, K. K. 1989, ApJ, 347, 835
Gilroy, K. K., & Brown, J. 1991, ApJ, 371, 578

Gratton, R. G., et al. 2001, A&A, 369, 87
Gratton, R. G., Sneden, C., Carreta, E., & Bragaglia, A. 2000, A&A, 354, 169
Grundahl, F., Briley, M., Nissen, P. E., & Feltzing, S. 2002, A&A, 336, 915
Iben, I., Jr. 1965, ApJ, 142, 1447
Ivans, I. I., Sneden, C., Kraft, R. P., Suntzeff, N. B., Smith, V. V., Langer, G. E., & Fulbright, J. P. 1999, AJ, 118, 1273
Maeder, A., & Zahn, J. P. 1998, A&A, 334, 1000
Mestel, L. 1953, MNRAS, 113, 716
——. 1957, ApJ, 126, 550
Palacios, A., Charbonnel, C., Bolmont, J., & Thévenin, F. 2002, Ap&SS, 281, 213
Palacios, A., Charbonnel, C., & Forestini, M. 2001, A&A, 375, L9
Palacios, A., Talon, S., & Charbonnel, C. 2004, in preparation
Palacios, A., Talon, S., Charbonnel, C., & Forestini, M. 2003, A&A, 399, 603
Pilachowski, C. A., Sneden, C., & Booth, J. 1993, ApJ, 407, 699
Ramírez, S. V., & Cohen, J. G. 2002, AJ, 123, 3277
Shetrone, M. 2003, ApJ, 585, L45
Sweigart, A. V., Greggio, L., & Renzini, A. 1989, ApJS, 69, 911
Sweigart, A. V., & Mengel, J. G. 1979, ApJ, 229, 624
Talon, S., Zahn, J. P., Maeder, A., & Meynet, G. 1997, A&A, 322, 209
Thévenin, F., Charbonnel, C., de Freitas Pacheco, J. A., Idiart, T. P., Jasniewicz, G., de Laverny, P., & Plez, B. 2001, A&A, 373, 905
Yong, D., Grundahl, F., Lambert, D. L., Nissen, P. E., & Shetrone, M. D. 2003, A&A, 402, 985
——. 2004, in Carnegie Observatories Astrophysics Series, Vol. 4: Origin and Evolution of the Elements, ed. A. McWilliam & M. Rauch (Pasadena: Carnegie Observatories, http://www.ociw.edu/symposia/series/symposium4/proceedings.html)
Zahn, J. P. 1992, A&A, 265, 115
Zoccali, M., Cassisi, S., Piotto, G., Bono, G., & Salaris, M. 1999, ApJ, 518, L49